REVIEWS

Flexible inorganic oxide thin-film electronics enabled by advanced strategies

Tianyao Zhang, Guang Yao[†], Taisong Pan, Qingjian Lu, and Yuan Lin[†]

State Key Laboratory of Electronic Thin films and Integrated Devices, University of Electronic Science and Technology of China, Chengdu 610054, China

---

Abstract: With the advent of human-friendly intelligent life, as well as increasing demands for natural and seamless human-machine interactions, flexibility and wearability are among the inevitable development trends for electronic devices in the future. Due to the advantages of rich physicochemical properties, flexible and stretchable inorganic oxide thin-film electronics play an increasingly important role in the emerging and exciting flexible electronic field, and they will act as a critical player in next-generation electronics. However, a stable strategy to render flexibility while maintaining excellent performance of oxide thin films is the most demanding and challenging problem, both for academic and industrial communities. Thus, this review focuses on the latest advanced strategies to achieve flexible inorganic oxide thin-film electronics. This review emphasizes the physical transferring strategies that are based on mechanical peeling and the chemical transferring strategies that are based on sacrificial layer etching. Finally, this review evaluates and summarizes the merits and demerits of these strategies toward actual applications, concluding with a future perspective into the challenges and opportunities for the next-generation of flexible inorganic oxide thin-film electronics.

Key words: flexible electronics; laser lift-off; van der Waals epitaxy; transfer printing

---

1. Introduction

Inorganic oxide thin films have attracted extensive attention thanks to their rich electrical, optical, thermal, mechanical, magnetic and other properties[1–8], which can be implemented into a variety of electronic devices and widely used in civilian and military fields. However, with the advent of artificial intelligence, virtual reality and the internet of things, traditional rigid oxide thin-film devices on a rigid substrate are unable to meet the urgent need for natural, seamless, and insensitive flexibility and wearability. Although several approaches have been proposed to make oxide thin films flexible, there are still many serious challenges to maintain the excellent performance of the oxide thin films during the process. For example, many researchers have tried to directly fabricate inorganic oxide films on flexible substrates (e.g., ultrathin glass and metal foil) and some thin polymer materials (e.g., polyethylene terephthalate (PET), polyimide (PI) and so on)[9, 10]. However, high quality inorganic oxide films usually require a high temperature treatment process, which is beyond the limits of the polymer. Even though ultrathin glass and metal foil can overcome the limitations of high temperature, they are fragile and costly. Therefore, there is an urgent need to exploit stable strategies to render flexibility while maintaining the excellent performance of oxide thin films.

Benefiting from the rapid development of materials, mechanics and manufacturing science, flexible oxide thin films have been enabled to achieve various deformations, such as bending[11–15], stretching[16] and twisting[17]. In addition, through structure design and device integration[18–20], oxide thin-film devices interconnected via serpentine lines[21, 22] or helical coils[23] have been designed to realize flexibility and wearability. This review covers recent advances in strategies for flexibility and recent major progress on novel applications of flexible inorganic oxide thin-film electronics, as shown in Fig. 1. First, laser lift-off (LLO) and van der Waal epitaxy are raised as the physical strategies, emphasizing their mechanical peeling characteristics. Next, a transfer-printing method based on sacrificial layer etching is introduced as the chemical strategy. The key design considerations (e.g., sacrificial layer, transferred velocity and substrate adhesion) are also discussed. Subsequently, this review summarizes the merits and demerits of these strategies in terms of thin film damage and strategic universality. Finally, the challenges and opportunities for the next-generation flexible inorganic oxide thin-film devices are discussed.

2. Physical strategies

Physical strategies refer to thin films that can be mechanically stripped to achieve macro-scale flexibility. LLO technique is a selective technology to remove one material from another[24–26]. Meanwhile, van der Waal epitaxy of thin films on micas provides another approach, in which the epitaxial layer can be easily directly peeled off because of the unique epitaxial growth nature[27–29].

2.1. Mechanical peeling through LLO

In the LLO technique, a transparent substrate is required to allow the laser beam to scan the entire interfacial film. Be-
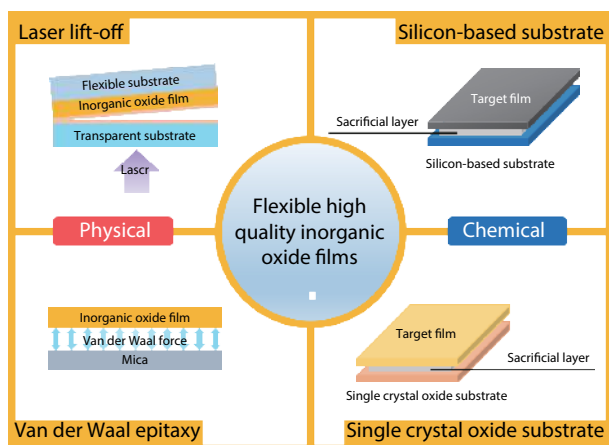
Fig. 1. (Color online) Advanced strategies for high quality inorganic oxide thin-film flexibility. In particular, the physical flexible strategies include LLO and van der Waal epitaxy, while the chemical flexible strategies include transferring films from silicon-based substrates and traditional single crystal oxide substrates to flexible substrates after etching the sacrificial layer.

cause the laser beam energy is lower than the band gap of substrate material and higher than that of upper film material, the laser beam energy can be absorbed only by the upper film, which results in damage-free separation of the upper film from the substrate[24, 26, 30]. Therefore, LLO provides an efficient, non-contacting and non-damage substrates replacement process. Moreover, to improve its generality and controllability, LLO has been developed to laser-induced forward transfer[31–33], laser-assisted bioprinting[34–37], laser-driven transfer printing[38, 39] and so on. This technique has been used to fabricate flexible memories[40], skin-like transistors[41], flexible light-emitting diodes (LED)[42–44], flexible generators[45, 46] and so on; as shown in Fig. 2. The LLO process is as follows. First, the film to be transferred is usually deposited on a transparent substrate. Then, the adhesion between the exfoliation layer and the donor substrate is reduced by laser irradiation. It should be noted that pulsed laser a short wavelength is usually used to reduce the thermal effect because of the high absorption and short interaction time, which can protect the transferred film. Finally, after the substrate has been entirely scanned by the laser, the film is separated from the donor substrate, which can then be attached to a flexible substrate[24, 30, 46].

Lee's group has fabricated flexible nanogenerator (NG) by growing the $PbZr_{0.52}Ti_{0.48}O_3$ (PZT) film by sol-gel method with a subsequent crystallization step at 650 °C on sapphire substrate[46]. The film was then separated from the sapphire substrate using the LLO technique and transferred to a plastic substrate. Next, interdigital electrodes were fabricated on the film. Thus, an efficient, flexible, lightweight, and large-area piezoelectric thin film nanogenerator was formed; as shown in Figs. 2(d)–2(h). This has a high output performance as the measured output voltage and current signals reach up to ~200 V and 150 μA/cm^2, respectively, during periodic bending/unbending motions (Fig. 2(g)). Furthermore, it allowed several blue LED arrays to be activated by slight bending motions of human fingers without any external electric power and circuits, as shown in Fig. 2(h). This enables us to develop self-powered flexible electronic devices for safety,

health, and environmental monitoring systems. To highlight the sensitivity of the structure, Lee's group has further fabricated a flexible inorganic piezoelectric acoustic nanosensor (iPANS) with a similar process, which can response to tiny vibration mimicking the function of hair cells (Fig. 2(i))[47]. The vibration information of the iPANS versus sound wave was investigated by attaching it onto a trapezoidal frequency separator and vibrating the frequency separator with a speaker. Fig. 2(j) shows the vibration displacement and vibration amplitude of the iPANS. The results indicate that the piezoelectric signal is in good correspondence to the vibration displacement, and the iPANS has little influence to the capability of frequency selectivity of the frequency separator. In addition, the vibration amplitude and piezoelectric potential are independent of frequency. There is no doubt that the concept of this iPANS expands the application of inorganic piezoelectric oxide in bionics.

The LLO technique can realize the large area transfer of thin films with low damage. In addition, the substrate (such as sapphire used in LLO technique) can be reused[48, 49]. However, as mentioned earlier, the LLO technique requires that the laser beam energy is lower than the band gap of substrate material and higher than that of upper film material, which severely limited the types of high quality epitaxial layers. In addition, it is easy to produce redundant fragments when transferring the patterned film, which could pollute the required patterns[26]. Moreover, the upper film needs to absorb the laser bean energy and generate thermal decomposition to separate from the substrate, which means that there must be consumption of epitaxial layer and this may affect the expected performance. At the same time, the uneven heating or cooling of the upper layer during laser irradiation may also affect the performance[50, 51].

2.2. Mechanical peeling by van der Waal epitaxy on mica

Micas are well-known phyllosilicates belonging to monoclinic structure. Muscovite (M-Mica) and fluorphlogopite (F-Mica) are common substrates in the thin film fabrication process. The M-Mica can be perfectly split along (001) plane by mechanical exfoliation, resulting in atomically smooth surface. M-Mica also possesses rich properties of chemical inertness, high transparency, and mechanical flexibility. The F-Mica has the similar properties to M-Mica, but it has lower flexibility than M-Mica, while its thermal stability is better than that of M-mica[52–54]. Adjacent layers interact by weak van der Waals bonds which makes it easy to peel off, resulting in a sample with mechanical flexibility[27]. Furthermore, the weak van der Waals interaction also exist between film and substrate, which can reduce the threading dislocations and enable the epitaxial layer to grow with its bulk lattice[28]. Various ferromagnetic, ferroelectric, piezoelectric and photoelectric flexible thin films and devices have been fabricated on micas, as shown in Fig. 3. Liu's group has prepared large-scale and high-quality $Ba_{0.67}Sr_{0.33}TiO_3$ dielectric thin films on F-Mica, fabricating the capacitor with $SrRuO_3$ (SRO) as the bottom electrode and Pt as the top electrode[55]. The capacitor shows a high relative dielectric constant (ε_r' > 1200) and low loss tangent (~ 0.16). In addition, a tunability of 67% at low frequencies is also noticed. Furthermore, it can maintain the values of ε_r', tan δ, and tunability after 12 000 bending cycles
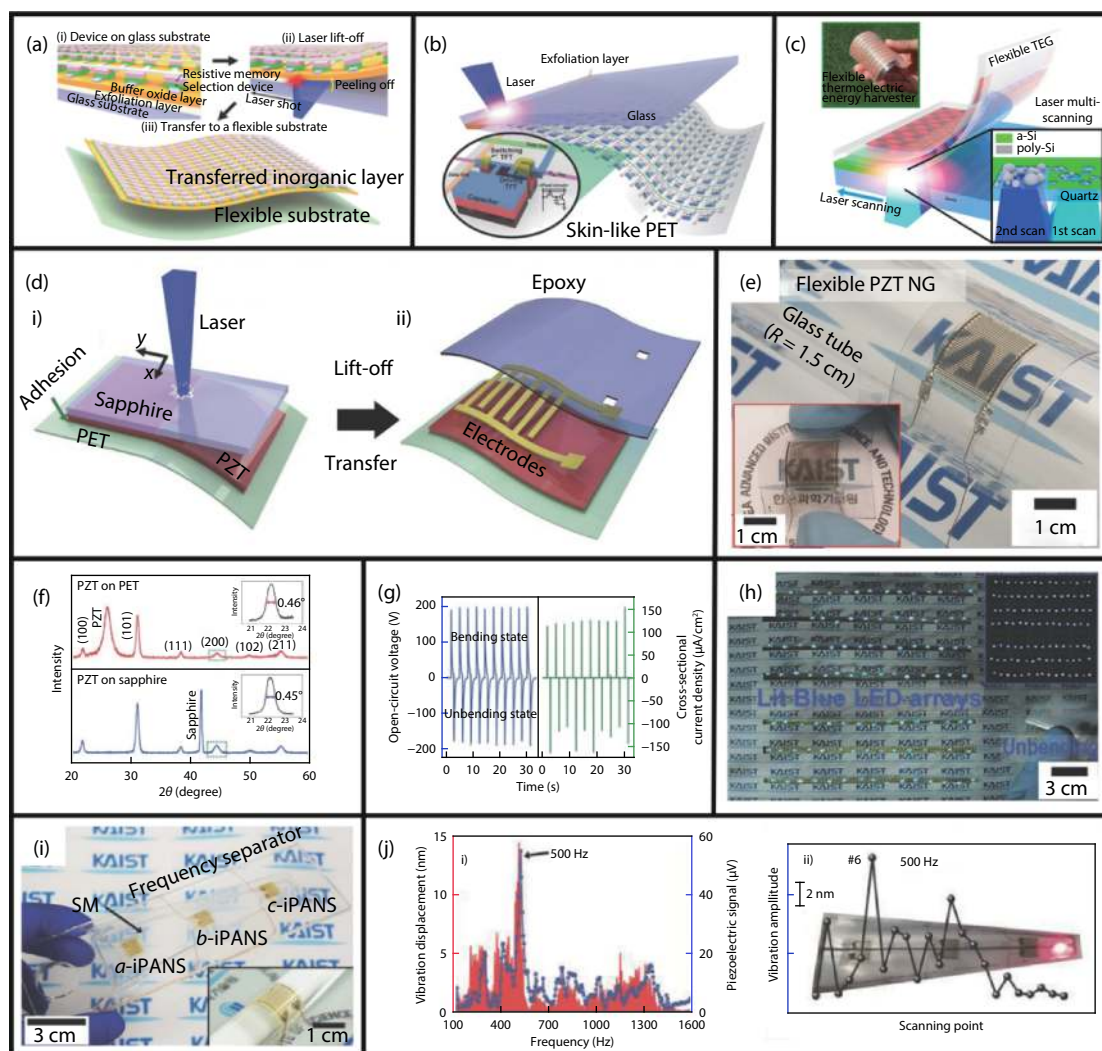
Fig. 2. (Color online) Mechanical peeling through LLO. (a–d) Schematic illustrations of the LLO process in fabricating flexible memory, skin-like transistor, thermoelectric generator, NG[40, 41, 45, 46]. (e) Photograph of the flexible PZT thin film-based NG attached to a glass tube, and the inset shows the bent NG[46]. (f) X-ray diffraction results of PZT thin films on a flexible (top, red) PET and a sapphire (bottom, blue) substrate[46]. (g) The open-circuit voltage and cross-sectional current density measured from PZT thin film-based NG in the forward connections[46]. (h) The instantaneous lighting up of 105 blue LEDs in series when an NG device is unbent after slight bending, and the inset shows the driven LED arrays in a darkroom[46]. (i) Photograph of the frequency separator with iPANS, and the inset shows a single iPANS unit attached to a glass rod with a radius of curvature of 1.0 cm[47]. (j) The vibration displacement i) and vibration amplitude ii) information of the a-iPANS versus to sound wave with a frequency range of 100–1600 Hz[47].

with bending radius of 5 mm. Chu's group has fabricated a flexible ferroelectric field-effect transistor (FET) on M-Mica with an aluminum-doped zinc oxide film as the semiconductor channel layer and a $PbZr_{0.7}Ti_{0.3}O_3$ film as the ferroelectric gate dielectric[56]. They have also prepared a flexible photoelectrode based on the heteroepitaxy of Fe_2O_3/ZnO/M-Mica, and its photo-electro-chemical (PEC) performance under different bending states has been investigated[57]. Compared to other substrates, micas can be mechanically cut thin enough due to the weak interaction between adjacent layers. Chu's group has prepared MoO_2 films on M-Mica and further obtained the free-standing MoO_2 thin films by removing the entire substrates as shown in Fig. 3(d)[29].

In the process of promoting device flexibility, the coupling between material properties and mechanical deformation should be of concern, including magnetostrictive properties, piezoelectric effects, and so on. Magnetostriction represents the relationship between the strain state and the magnet-

ic state of a ferromagnet, which can be quantified by magnetostrictive coefficient (λ). To achieve higher response to magnetic field, Chu's group has grown van der Waals epitaxial $CoFe_2O_4$ (CFO) thin films on M-Mica by the pulsed laser deposition (PLD) method. The reflective high energy electron diffraction (RHEED) is adopted to in situ monitor the deposition[58]. Fig. 3(a) shows the schematic of the deposition process. They found that the hysteresis loops were basically the same under different bending conditions, and the saturation magnetization can be maintained at 120–150 emu/cm³, whereas the difference of magnetostriction coefficient (Δλ) versus the sample length is –104 ppm. Moreover, Chu's group has grown Fe_3O_4 thin films on M-Mica by ultrahigh vacuum molecular beam epitaxy (MBE) and carried out various bending tests[59]. The results indicate that the saturation magnetization, remanent magnetism, and coercivity of Fe_3O_4 films can be retained during bending, while the easy axis rotated gradually from the in-plane direction to the out-of-plane direction
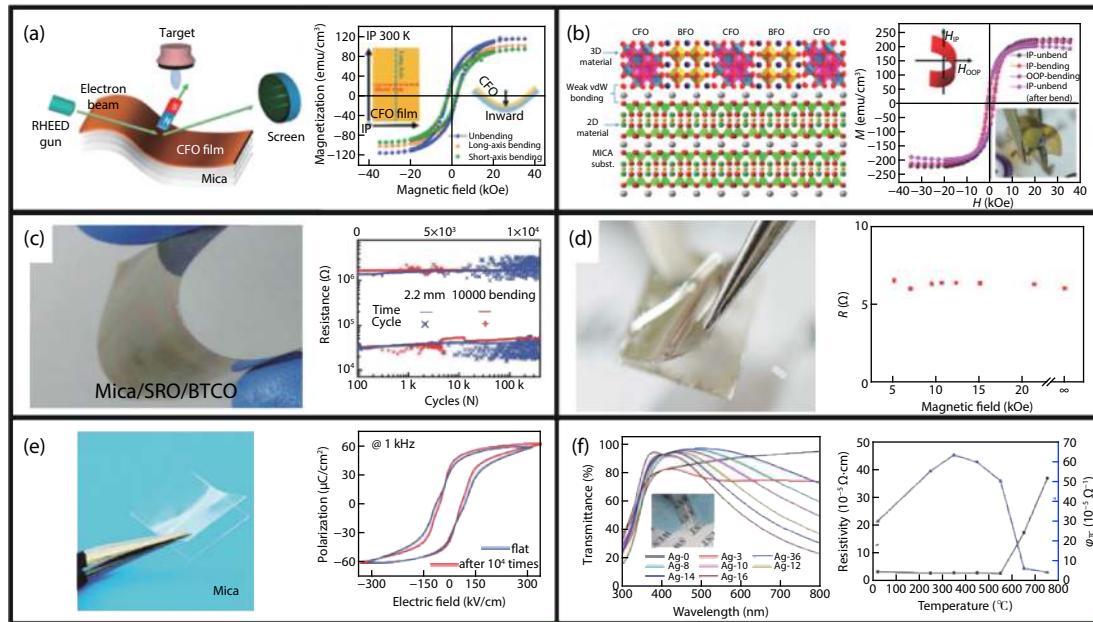
Fig. 3. (Color online) Mechanical peeling by van der Waal epitaxy on mica. (a) Schematic of deposition process for flexible CFO film monitored by RHEED in real time (left), and the magnetic hysteresis loops (right) show that the flexible CFO/mica exhibits solid magnetic properties regardless of bending[58]. (b) Crystal structure of the interface region between the CFO–BFO composite and mica substrate (left), and the M–H loops of BFO–CFO under bending conditions (right) are in agreement with the flexible CFO/mica[63]. (c) Optical images of bending mica/ SRO/BTCO (left) which shows great resistance switch characteristics (right)[64]. (d) MoO_2/M-Mica can remain the resistance under different bending radii (right), and the whole MoO_2 film can be removed from M-Mica (left)[29]. (e) Photo of mechanical peeling 10-μm-thick mica (left) and P–E loops before and after the PZT film being bent to bending radius of 2.2 mm for 10^4 times[65]. (f) The flexible and transparent AZO/ Ag (8 nm)/AZO multilayer films (left) shows great resistivity (right) and transmittance even after annealing at 750 °C[72].

with a decrease in the magnetic. anisotropy. They attributed these phenomena to the magnetostriction of Fe_3O_4. In addition, a flexible FET structure with in-situ low voltage control was developed on F-Mica by Liu's group[60]. By applying low voltage to the control layer (ionic gel), the spin dynamic characteristics of the functional layer (Fe_3O_4) are manipulated, which can achieve a reversible non-volatile 345 Oe ferromagnetic resonance (FMR) field shift corresponding to the large magnetoelectric (ME) coefficient of 230 Oe/V. During the bending test, a reversible 126 Oe FMR field shift corresponding to the ME coefficient of 84 Oe/V is obtained at the curvature radius of 15 mm. Liu's group explained that the ionic transition between Fe^{2+} and Fe^{3+} at the interface induced by electric field is the reason for the tunable ME. Specifically, the ratio of Fe^{2+}/Fe^{3+} in the functional layer can be changed with Fe^{3+} change to Fe^{2+} by gaining an electron. Moreover, Liu's group has grown $Li_{0.35}Zn_{0.3}Fe_{2.35}O_4$ films on F-Mica by PLD method[61]. The highly stable in-plane (IP) FMR spectra and tunable out-of-plane (OOP) FMR spectra are observed in the films during bending test. Meanwhile, the films after 10^4 bending cycles at a radius of 5 mm have the basically same FMR character as the original sample, which exhibit high mechanical fatigue resistance. Furthermore, Liu's group has grown $CuFe_2O_4$ films on F-Mica, and it is observed that the tension strain and compression strain have obvious effects on the in-plane FMR resonance field[62]. All of these flexible epitaxial magnetic films with tunable microwave magnetism and good mechanical durability have wide application prospects in flexible spintronics, microwave detectors, mechanical magnetic sensors, and so on.

The clamping effect caused by rigid substrate has al-

ways been an important factor to weaken the magnetoelectric coupling. To overcome this problem, Chu's group has prepared van der Waals epitaxy self-assembled $BiFeO_3$ (BFO)-CFO bulk heterojunctions on M-Mica[63]. Because the bulk heterojunction interacts with the substrate by weak van der Waals force (Fig. 3(b)), the interface is not coherent and this greatly reduces the clamping effect. The ME coupling coefficient of the bulk heterojunctions can reach to 74 mV/(cm·Oe), and the magnetic hysteresis loop remains unchanged before and after bending at bending radius of 2 mm.

A flexible memory unit is an important part of flexible display screens and smart wearable devices. Although organic memory is more flexible than inorganic memory, it generally has poor high temperature stability and is easy to oxidize under illumination. Thus, it is important to develop inorganic memory with mechanical flexibility and high temperature stability. Chu's group has grown van der Waals epitaxial $PbZr_{0.2}Ti_{0.8}O_3$ thin films on M-Mica[10]. As a non-volatile memory device, it not only has good reliability and thermal stability but also exhibits excellent mechanical performance under bending condition of bending radius less than 2.5 mm and 10^3 bending cycles. It is worth noting that before depositing SRO layer as the bottom electrode on mica, CFO buffer layer with less than 10 nm was deposited as the seeding layer for growing high quality SRO layer, and the SRO electrode layer could prevent the severe fatigue behavior of polarization which is often encountered in PZT capacitors with metal electrodes. Moreover, Liu's group has prepared $BaTi_{0.95}Co_{0.05}O_3$ (BTCO) on 10-μm-thick F-Mica with the SRO buffer layer[64]. They found that either after the memory was written/erased for 360 000 cycles at bending radius of 1.6 mm, or after the

memory was bent to bending radius of 3 mm for 10^4 times, there was no significant change in the resistance switch characteristics, as shown in Fig. 3(c). To obtain piezoelectric thin films with high piezoelectricity and good flexibility at the same time, Liu's group has fabricated a flexible capacitor by growing SRO, PZT, Pt films on 10-μm-thick F-Mica, as shown in Fig. 3(e)[65]. The capacitor exhibits an amplified longitudinal piezoelectric d_{33} of about 1200 pm/V with a saturated polarization of around 60 μC/cm^2 and a dielectric tunability of around 90%. There was no obvious change in polarization, dielectric tunability, or piezoelectric response after being bent to bending radius of 2.2 mm for 10^4 times. In addition, Liu's group grew La$_{0.67}$Sr$_{0.33}$MnO$_3$/SrTiO$_3$ (LSMO/STO) double layer on F-Mica by the PLD method, and then grew BaZr$_{0.35}$Ti$_{0.65}$O$_3$ (BZT) film on the double layer by radio frequency magnetron sputtering, fabricating a large-scale BZT capacitor[66]. The recoverable energy density (W_{rec}) and efficiency (η) of the capacitor exceed 65.1 J/cm^3 and 72.9% in the ultrawide temperature range of –100 to 200 °C. The capacitor can maintain W_{rec} of above 69.4 J/cm^3 and excellent η above 84.7% at 6.15 MV/cm even after 10^4 bending cycles and 10^6 ferroelectric fragile cycles. Moreover, they replaced the LSMO/STO double layer by Sn-doped In$_2$O$_3$ (ITO), fabricating another BZT capacitor, which could work properly in the range of –120 °C to 150 °C. There was no obvious change both in W_{rec} and η after 10^4 bending cycles[67]. Furthermore, they replaced the BZT film by BaTiO$_3$ (BTO) film, which exhibited a high retention of ferroelectric polarization of 96.41% after 10^6 electric field cycling and 92.64% after 10^4 mechanical fatigue cycles at the bending radius of 6 mm, respectively[68]. These results demonstrate that the flexible dielectric capacitors have potential applications for flexible wearable electronics in wide-temperature and harsh working environments.

Transparent conducting oxides (TCO) have been widely used in solar cells, light emitting diodes, photodiodes, thin film transistors, photocatalysis, flat panel displays, gas sensors and energy-saving windows, and have become the basic components of advanced technology and equipment. With the development of portable and flexible electronic devices, it is particularly important to find a transparent and mechanically flexible base for TCO. As mentioned earlier, the commonly used transparent and flexible substrates are problematic; for example, ultra-thin glass is fragile and expensive, while polymer substrates such as PET and PI are not thermally stable, which impedes the growth of high-quality films. Meanwhile, micas are the ideal substrate for TCO preparation because of their high transparency, smooth atomic surface, thermal stability, chemical stability, flexibility, and mechanical durability. Chu's group has grown van der Waals epitaxy TCO including ITO and Al-doped ZnO (AZO) films on M-Mica. A yttria-stabilized zirconia (YSZ) buffer layer was deposited before the ITO deposition, which is confirmed later that YSZ/mica heterostructure has good ionic conductivity and a high transmittance of more than 90% in the visible (380–800 nm) range[69]. The properties of TCO fabricated by them are similar to those fabricated on rigid substrates. The conductivity of TCO/M-Mica increases with the increase of TCO thickness. These TCO electrodes exhibited good chemical and thermal stability and mechanical durability[70]. In addition, Huang's group has deposited high quality ITO films on M-Mica[71]. The ITO/M-Mica

showed a fast rise time (< 15 s) to reach 90% of the steady-state temperature, and it was able to maintain the low resistivity after 10^3 consecutive bends. These epitaxial TCO electrodes could greatly promote the development of flexible and portable smart electronics. To broaden the possibilities of flexible optoelectronics with stable electrical properties and reliable optical properties, Wei's group has fabricated AZO/Ag/AZO multilayer on F-Mica by radio frequency magnetron sputtering, as shown in Fig. 3(f)[72]. They were able to maintain a stable resistivity under 550 °C. After annealing at 750 °C, it also showed the resistivity of 3.69 × 10^{-4} Ω·cm and transmittance of 87.0%. Furthermore, Liu's group has fabricated ITO/Ag/BTCO/Ag-ITO on F-Mica, with a high/low resistance ratio of 5000 and fast response speed around 50 ns[73]. The high or low resistance states remained stable after 5000 bending cycles at a radius of 2.2 mm or 14 400 bending cycles at a radius of 3 mm. Obviously, micas offer more potential opportunities for developing flexible and transparent high-performance electronic devices.

In summary, micas can be widely used in various flexible devices. Generally, M-Mica has higher transparency, slightly better electrical properties and better flexibility than F-Mica, while F-Mica has better thermal stability than M-Mica, thus F-Mica is more suitable for the films which need higher annealing temperature for better crystallinity, and M-Mica is more suitable to increase the flexibility of films or devices. However, even though the advantages of micas enable the epitaxial layer to grow with its bulk lattice, it can hardly control the orientation of epitaxy layer, thus a thin buffer layer on the surface of mica or surface treatment for mica is usually needed[10, 28, 56, 59, 63, 66, 68, 70, 74].

3. Chemical strategies

For chemical strategies to make flexible thin film devices, the basic idea is transferring films from rigid substrates to flexible substrates after etching the sacrificial layer. In 2004, Rogers's group first proposed microstructured silicon (μs-Si) technology, which involves photolithography, dry etching, wet etching and transfer printing process[75]. Photolithography and dry etching can pattern materials, and further wet etching is to obtain free-standing patterned films. Then the patterned films can be fabricated on flexible substrate after transfer printing process. In addition, Rogers's group has made similar attempts on other semiconductors, developing μs-Si technology into microstructured semiconductor (μs-SC) technology[76]. The advantage of this technology is that before transferring patterns, semiconductor materials can be doped, deposited, and annealed at high temperature. At the same time, the shape, size, and spatial position of patterns can be precisely controlled, which greatly promotes the development of high-performance flexible electronic systems. A schematic illustration of the generic process flow for transfer printing is shown as Fig. 4(a)[77]. Because the strength of adhesion between the film and the stamp greater than that between the film and the donor substrate, film can be peeled off from the donor substrate by the stamp. Conversely, by controlling the strength of adhesion between the film and the stamp to less than that between the film and the receiving substrate, the stamp can be peeled off while leaving the film on the receiving substrate. The donor rigid substrates include silicon-based substrates commonly used in electronic
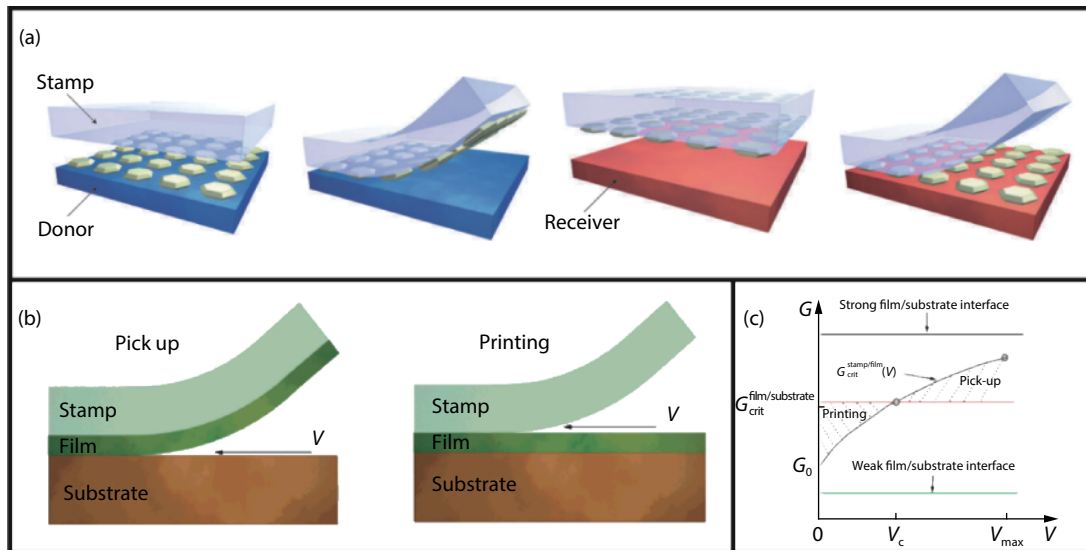
Fig. 4. (Color online) Transfer printing technology. (a) Schematic illustration of the generic process flow for transfer printing[77]. (b) Schematic diagrams of pick up (left) and printing (right) of a thin film[78]. (c) Schematic diagram of critical energy release rates for the film/substrate interface and for the stamp/film interface[78].

devices and traditional single crystal oxide substrates. The silicon-based substrates are mainly monocrystalline silicon, silicon on insulators (SOI), III–V semiconductors, and so on.

Rogers's group and Huang's group have analyzed the dynamic control of the adhesive force of elastic stamps[77, 78]. The adhesion force can be expressed by the critical energy release rate between the film and the substrate or stamp, and the relative magnitude of the critical energy release rate between the stamp and the film ($G_{crit}^{stamp/film}$) and the critical energy release rate between the film and the substrate ($G_{crit}^{film/substrate}$) determines the peeling and printing of the transfer process. They believe that $G_{crit}^{stamp/film}$ is an increasing function of the peeling rate, while the energy release rate between the film and the substrate is independent of the peeling rate. As shown in Fig. 4(c), there is a critical peeling rate v_c between peeling and printing. When reference peeling rate v is larger than v_c, the $G_{crit}^{stamp/film}$ is larger than $G_{crit}^{film/substrate}$, resulting in peeling process, while the printing process is achieved when v is less than v_c. In particular, for weak film/substrate interface, the film will only be picked up. For strong film/substrate interface, the film will only be printed. With the development of transfer printing technology, several strategies for controlling adhesion during transferring process have been proposed, such as kinetic control, surface-relief-assisted control, load-enhanced control, laser-driven control, and shape memory driven control[79].

3.1. Transferring of oxide thin films grown on silicon-based substrates

Based on μs-SC technology, Lee's group has deposited BTO films on prepared Pt/Ti/SiO$_2$/Si substrate by radio frequency magnetron sputtering, following by annealing process above 600 °C[80]. The Ti layer is oxidized to TiO$_2$ layer for subsequent wet etching. Finally, a layer of Au is coated on the surface of BTO to form a metal–insulator–metal (MIM) capacitor structure, as shown in Fig. 5(a). Fig. 5(b) shows that the flexible MIM capacitor is obtained by transferring it to the plastic substrate using PDMS as the stamp. Fig. 5(c) shows

the bending test results, indicating that its dielectric constant does not change significantly with the change of bending radius from 1.93 to 0.84 cm (corresponding to surface strain of 0.32 to 0.74%), which shows the high mechanical stability of flexible dielectric device upon harsh bending. In addition, Lin's group has fabricated transparent photodetectors based on ITO/Si heterojunction on flexible PET substrates using polymethyl methacrylate (PMMA) assisted transfer printing technology, and systematically studied the band structure of the heterojunction, and the relationship between the detector performance and bending deformation, as shown in Figs. 5(d)–5(f)[81]. The ITO/Si heterojunction was prepared by depositing ITO on SOI substrate with radio frequency magnetron sputtering system, following by an annealing process. Finally, the ITO/Si heterojunction structure was transfer-printed to the PET substrate with ITO thin film electrodes and Au thin film electrodes to complete the construction of flexible ITO/Si heterojunctions. The results show that by applying bending strain to ITO/Si heterojunction, the height of interface barrier and the response time of photodetectors based on the heterojunction can be continuously reduced, which provided a new idea for the integration of high-performance flexible photodetectors. To increase the tensile properties of PZT inorganic oxide films, Feng's group has transfer-printed the PZT nanoribbons prepared on SiO$_2$ substrates to the pre-stretched PDMS substrates to form stretchable wavy structures, as shown in Figs. 5(g)–5(i)[82]. The results show that corrugated PZT nanoribbons had the same ferroelectric and piezoelectric properties as those on rigid silicon substrates. In addition, they showed that with the increase of tensile strain, the wavelengths of the sinusoidal shape increase and the amplitudes of that decrease, and because of piezoelectric effect the amplitude of the PZT nanoribbons can be continuously adjusted under the action of an applied electric field. LiNbO$_3$ (LNO) is an important material for optical waveguides, mobile phones, piezoelectric sensors, optical modulators, and other linear and non-linear optical applications. In contrast to obtaining free-standing thin films on silicon substrates by remov-
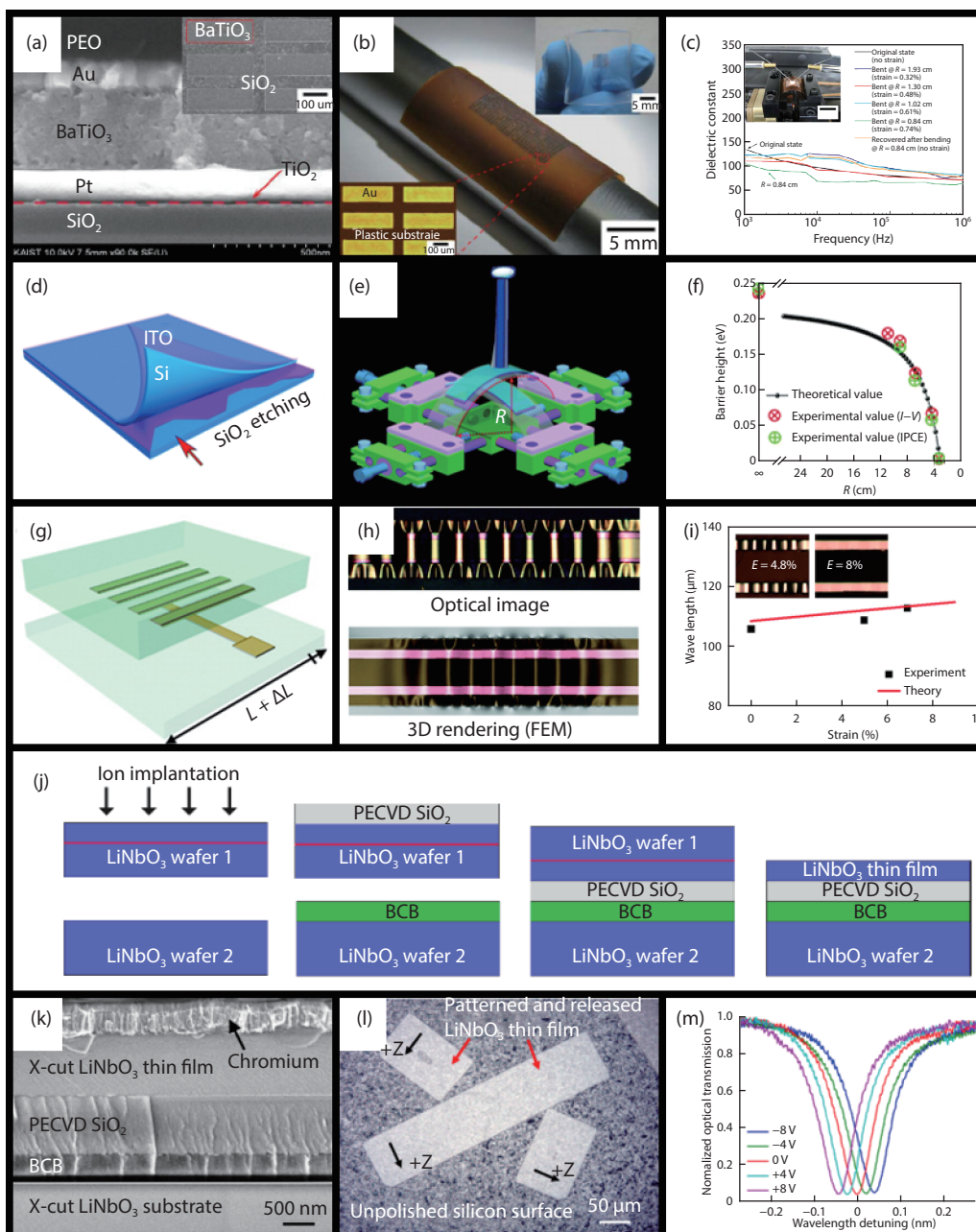
Fig. 5. (Color online) Transferring of oxide thin films grown on silicon-based substrates. (a–c) A cross sectional image (a), optical image (b) and dielectric properties (c) of the bendable PEO/Au/BTO/Pt/TiO$_2$/SiO$_2$/Si structure[80]. (d–f) Schematic illustration of etching SiO$_2$ for flexible ITO/Si structure (d) and the measurement of the photodetector (e), and the barrier height of the bent ITO/Si heterojunction versus its bending radius (f) shows that the barrier height decreases with the bending radius[81]. (g–i) Schematic illustration of printing transfers the PZT nanoribbons to the pre-stretched PDMS (g), and the optical image and three-dimensional (3D) rendering of wavy PZT nanoribbon devices on PDMS (h), which the measured wavelength of wavy PZT nanoribbons as a function of applied tensile strain fits well with that of theory (i)[82]. (j) Schematic illustration of ion-sliced LNO exfoliation[83]. (k–m) SEM of the cross-section (k) and the transfer surface (l) of the LNO thin film, and the wavelength detuning with voltage as parameter of Si/LNO racetrack resonator (m)[83].

ing the silicon substrates in etching step, LNOs are mostly prepared with a SiO$_2$ interlayer on LNO single crystal, whose process is similar to smart cut SOI as shown in Fig. 5(j)[83]. The free-standing LNO substrate can be obtained by etching the SiO$_2$ interlayer. Figs. 5(k)–5(m) shows a tunable resonator with coplanar electrodes by this method, which has a tunability of 5.2 PM/V.

Metal–insulator transition (MIT) refers to the phenomenon of transforming or reversing from metal to insulator under certain external conditions, which has attracted consider-

able attention. Vanadium dioxide (VO$_2$), as a well-known MIT material, will change from insulating monoclinic phase at low temperature to metal tetragonal phase at high temperature, and its optical and electrical properties will change dramatically at the same time. Its phase transition temperature (T_c) is close to room temperature and the resistance difference before and after phase transformation can reach 10^5. Moreover, VO$_2$ has a high temperature coefficient of resistance (TCR) near room temperature, so it is very suitable for sensitive materials in temperature sensors. Lin's group has prepared VO$_2$
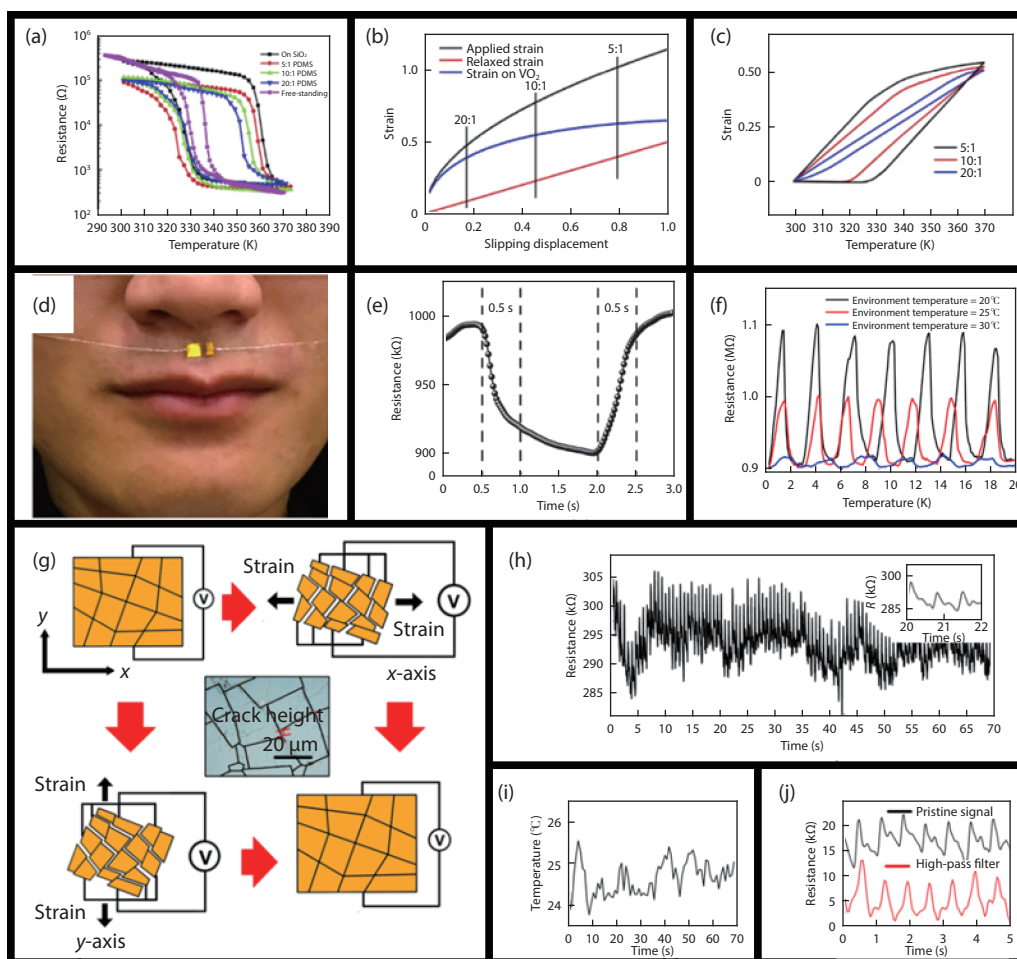
Fig. 6. (Color online) Flexible sensors based on VO$_2$/PDMS structure. (a) The resistance versus temperature curves for the VO$_2$ film in different states[85]. (b) Applied strain, relaxed strain and strain on VO$_2$ at different slipping displacements[85]. (c) Strain on VO$_2$ under heating and cooling cycles[85]. (d) The photograph of the breath sensor based on PI/VO$_2$/PDMS structure[86]. (e) Response time and recovery time to breath[86]. (f) Resistance changes at different environment temperatures[86]. (g) Schematic illustration of electrical conductance of the sensor and the behavior of the disconnection-reconnection when applied strain on the x-axis (transverse) and y-axis (longitudinal)[87]. (h–j) Real-time monitoring signals (h), temperature signals (i) and pulse signals (j) of the flexible temperature-strain composite sensor[87].

thin films on SiO$_2$/Si substrates by the polymer-assisted deposition (PAD) method[84–91]. They then transfer-printed VO$_2$ thin films on PDMS by PMMA assisted wet transfer method and heat release transfer printing technology, and so on. They investigated the effect of strain on MIT effect for VO$_2$/PDMS structure[85]. They have also successfully transferred VO$_2$ thin films with thickness of 130 nm to PDMS substrates with thickness of 1 mm and ratio of 5 : 1, 10 : 1, 20 : 1, respectively. The phase transition characteristics of VO$_2$ thin films have been measured in the temperature range of 300 to 370 K. As shown in Fig. 6(a), with the change of PDMS mixing ratio, the phase transition temperature T_c can be manipulated. This is because the coefficient of thermal expansion (CTE) of PDMS is much higher than that of VO$_2$, and tensile stress will occur during the heating process of resistance measurement, which will cause the change of T_c. With the increase of mixing ratio, the Young's modulus and CTE value of PDMS decrease, which causes that the tensile strain of VO$_2$ film decreases during the heating process. The data indicated that external strain induced by the stretchable structure could tailor the phase transition of the VO$_2$ thin films. After revealing the effect of strain on the MIT properties of VO$_2$ thin films, Lin's group has fabric-

ated a series of flexible sensors based on VO$_2$/PDMS structure, which has good adhesiveness and cyclicity of deformation, as well as comparable response speed and sensitivity with rigid electronic devices[86, 87].

Benefiting from the high TCR of VO$_2$ near room temperature, Lin's group has designed and fabricated a flexible breathing sensor with ultra-fast response based on PI/VO$_2$/PDMS structure[86]. They transferred VO$_2$ films to Au-plated PI using heat release transfer printing technology after patterning VO$_2$ films on SiO$_2$/Si substrates, and then packaged them with PDMS to make a breath sensor. The skin-like PDMS layer can achieve non-irritating skin adhesion, while the PI layer can effectively isolate the VO$_2$ material from the external strain to avoid the interference of body movement and other factors on respiratory monitoring. The sensor was naturally attached under the nostril (Fig. 6(d)), and the temperature changes caused by the breathing air flow at the nostril were monitored in real time to reflect the breathing state. Figs. 6(e) and 6(f) shows the results, showing that the response time and recovery time of the flexible breath sensor are both as fast as 0.5 s, and it has high sensitivity and stability. Inspired by the structure of spiders' slit sensilla[92], Lin's group has also tried
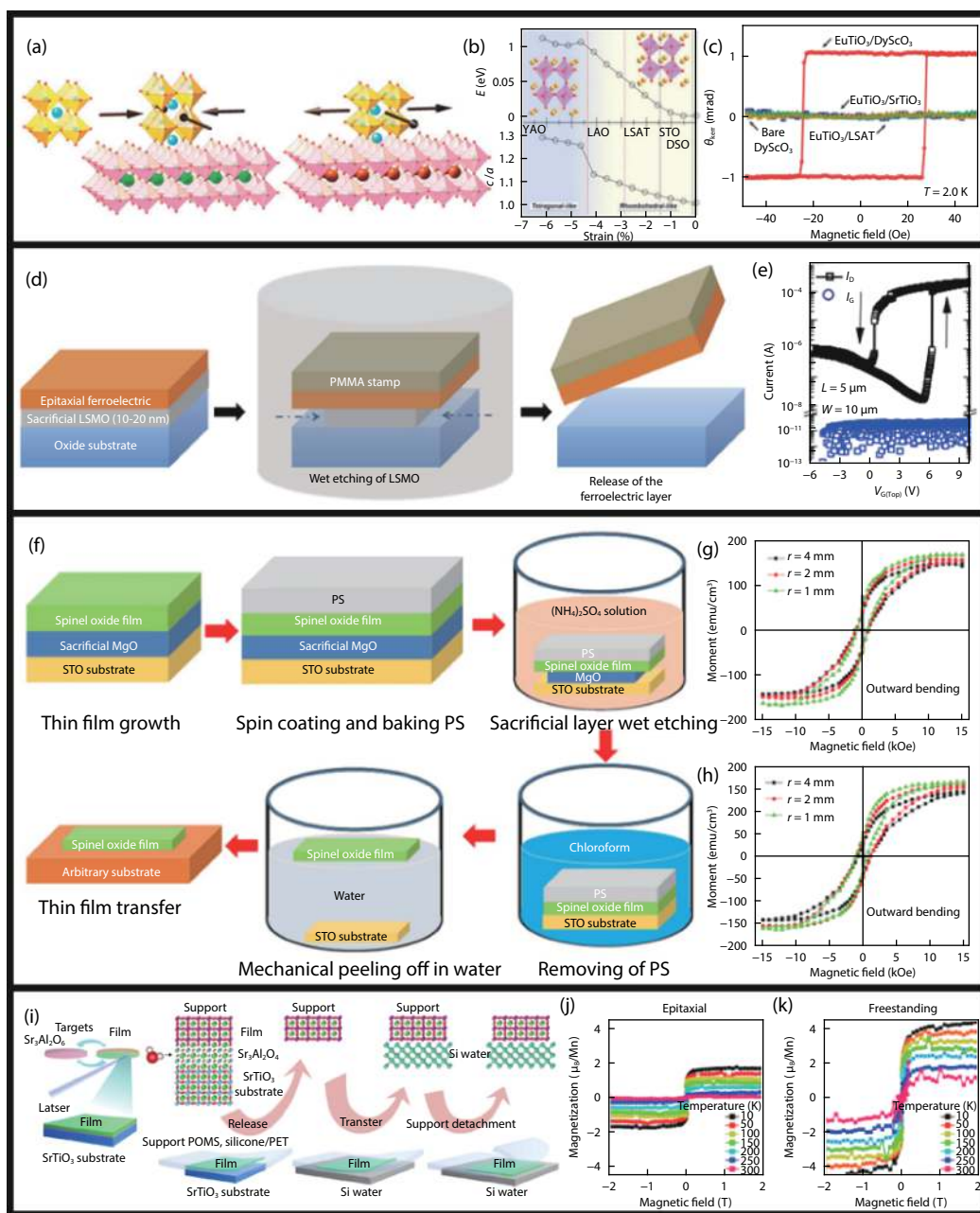
Fig. 7. (Color online) Transferring oxide thin films grown on traditional oxide substrates. (a) Crystal structure of biaxial compression and stretching process during depositing films on substrate with a smaller or larger lattice[93]. (b) The strain induced by substrates as BFO films grown on different substrates[93]. (c) The magneto-optical effect of the same strain ETO grown on (110) DSO substrate, which proves that ETO becomes multiferroic under sufficient biaxial strain[93]. (d) Schematic illustration of transferring PZT by etching LSMO as a sacrificial layer[96]. (e) The I_D–V_G (top gate) characteristics of the ferroelectric PZT-gated transistor at V_G (back gate) = 0[96]. (f) Schematic illustration of transfer processes of CFO thin films on flexible substrates[100]. (g, h) IP (g) and OPP (h) M–H hysteresis loops of the CFO thin films measured by vibrating sample magnetometer under different outward bending strains[100]. (i) Process schematic for heterostructure growth, oxide membrane release and transfer[102]. (j, k) IP magnetization loops of the SL (j) before and (k) after release[102].

to impose controllable tensile stress on VO_2 thin films on PDMS to form transverse and longitudinal zigzag cracks in advance and to detect the strain by the resistance change caused by crack displacement under strain[87], as shown in Fig. 6(g). Because VO_2 can also reflect the temperature change by resistance change, Lin's group has fabricated a flexible temperature-strain dual parameter sensor based on VO_2 thin film with transverse and longitudinal zigzag cracks. The responses of the sensor to heat and cold stimuli are within 0.5 s, and the gauge factor in the range of 0–0.1% strain is

over 400. Moreover, in practical application scenarios (such as simultaneous monitoring of body surface temperature and pulse signals), these authors studied the extraction of body surface temperature signals and pulse signals from a single resistance change information, as shown in Figs. 6(h)–6(j). Through the frequency analysis of the collected signals, they found that the surface temperature signal is a low frequency signal with variable frequency, while the pulse signal is a high frequency signal with higher amplitude than the surface temperature signal. Therefore, a surface temperature sig-

nal with frequency less than 1 Hz can be obtained by low-pass filtering, whereas the pulse signal can be obtained by high-pass filtering. Their resistance curve can then be obtained by inverse fast Fourier transform (IFFT).

The transfer based on silicon-based substrates is compatible with the modern electronic industry. However, it is also obvious that epitaxial growth of most of the oxide thin films on silicon-based substrates is difficult because of the amorphous nature of the SiO_2 layer. Therefore, it is very important to extend the transfer-printing technology used in silicon-based substrates to other single crystalline oxide substrates.

3.2. Transferring oxide thin films grown on single crystalline oxide substrates

With the development of strain engineering, researchers have done a lot of work on introducing large biaxial strain through heteroepitaxy. As shown in Fig. 7(a), following the energy preference of the substrate material or the lower layer epitaxial material, when the film material is deposited on the substrate with a larger lattice constant, the deposited atoms can cause the film to begin biaxial stretching. In contrast, when the film material is deposited on the substrate with a smaller lattice constant, the deposited atoms can cause the film to start biaxial compression[93]. In addition, the difference of thermal expansion coefficients between thin films and substrates can also introduce strain. The introduction of epitaxy strain can not only stretch or compress the atomic spacing in the film structure but can also lead to further changes in the composition, microstructure or crystal structure of the film[94]. Fig. 7(b) shows the functional relationship between ground state energy and structure of BFO films grown on different substrates and the strain induced by substrates[93]. While Fig. 7(c) shows the magneto-optical effect of the strained $EuTiO_3$ (ETO) grown on (110) $DyScO_3$ (DSO) substrate, which proves that ETO becomes multiferroic under sufficient biaxial strain[93]. However, due to the limited types of substrates produced in the market, it is difficult to implement continuous stress regulation for thin films based on traditional epitaxial strain engineering.

In recent years, many researchers have tried to transfer inorganic oxide films grown on single crystalline oxide substrates to other substrates using the approach of growing and etching a sacrificial layer. The sacrificial layers on single crystal oxide substrates correspond to the different etching solutions, which are often buffer solutions of different acids and salts[95]. The sacrificial layer must be lattice matching to the substrate and the film to ensure the epitaxial growth. Thus, searching on sacrificial layer materials is valuable. Ramesh's group has successfully transferred PZT grown on STO substrates to Si by PMMA-assisted wet transfer, as shown in Fig. 7(d)[96]. Its ferroelectric domains can be reversibly polarized by applying opposite electric fields. On this basis, they have fabricated single crystal PZT gated silicon transistors, and successfully proved that PZT is integrated into silicon devices. In the study of flexible single crystal $LiFe_5O_8$ (LFO) thin films to avoid chemical contamination caused by coating carrier layer, such as PMMA, during transfer printing and cracks caused by their subsequent dissolution, Liu's group has tried to attach PI tape to the surface of the thin films before etching sacrificial layer[97]. The results show that for LFO films with different thickness, there is no obvious damage

after transferring by this method. In the subsequent bending cycle test and magnetic test, LFO films also showed excellent flexibility and stability. LSMO was used as the sacrificial layer in these experiments, and the etching solution was a mixture of KI, HCl and H_2O. With different mixing ratios, the etching speed also varied. Generally, the higher the HCl content, the faster the etching speed, but too high pH value may also affect the inorganic oxide film, which is not strong acid-resistant.

After successfully transferring inorganic oxide films grown on single crystalline oxide substrates, researchers have found that the properties of inorganic oxide films can also be tailored with the stress regulation of flexibility, tension and torsion of inorganic oxide films transferred onto flexible substrates. Qi's group has prepared PZT nanoribbons on MgO substrates[98, 99]. After immersing them in 20% phosphoric acid at 120 °C for 50 s, the PZT nanoribbons could be transferred directly through PDMS. Subsequently, its potential application as an efficient electromechanical energy converter was confirmed by testing its basic piezoelectric properties. Furthermore, Qi's group has expanded the application scope of PZT by transferring it to pre-stretched PDMS substrates to form corrugated structures. In addition, Liu's group has used MgO as sacrificial layer and polystyrene (PS) as carrier to obtain freestanding CFO films from STO substrates, as shown in Fig. 7(f)[100]. The CFO films could be transferred to PI, and different degrees of uniaxial strain could be introduced into CFO films by bending PI to different degrees. Unlike traditional strain engineering, the critical thickness limitation, the change of crystal quality and the clamping of the substrate are avoided. They have found that the saturation magnetization and coercivity of CFO were strongly related to the bending radius of PI, as shown in Figs. 7(g) and 7(h). This has confirmed that the magnetic properties of oxide films can be adjusted by large and controllable external mechanical strain induced by flexible structures. In these studies, it can be seen that MgO as sacrificial layer can not only be etched by phosphoric acid but also $(NH_4)_2SO_4$ solution. Similarly, the concentration greatly affects the etching speed.

Unlike etching with acid or acid salt solutions, $Sr_3Al_2O_6$ (SAO) as sacrificial layer can be etched by water. Nie's group has prepared free-standing BFO film with atomic layer thickness by etching the water-soluble SAO buffer layer, which opened the door of two-dimensional quantum phenomena with strong correlation[101]. Hwang's group has deposited SAO buffer layer on STO, and then deposited single crystal STO, LSMO, and STO/LSMO superlattices (SL) on it, respectively[102]. Then, STO, LSMO and the superlattices were transferred to Si wafer with PDMS stamp by etching SAO layer, as shown in Figs. 7(i)–7(k). Compared with epitaxial films on rigid substrates, they believed that strain relaxation during film release has a significant impact on the physical properties of films. To improve the performance of magnetic oxide films in spintronics devices, Liu's group has transferred LSMO epitaxial films with different thickness (7, 15, 50, 100 nm) prepared on STO substrates with SAO as the sacrificial layer to PDMS[103]. The effects of different bending states on the microwave magnetic properties of these films were also studied. They found that, in FMR measurements, LSMO films with thickness greater than 7 nm exhibited anisotropy except for

LSMO films with thickness of 7 nm, and their anisotropy increased with the increase of thickness. In addition, they believe that as long as the direction of the applied magnetic field is adjusted, the constant and continuous tuning of ferromagnetic resonance field under different mechanical bending can be achieved in the same sample. Realizing the superelasticity and flexibility of ferroelectric thin films is a critical problem for applying ferroelectric materials in flexible electronic devices. Liu's group and Ding's group have achieved freestanding BTO thin film from STO substrates with SAO as the sacrificial layer, and an in situ bending test was carried out on it[104]. Their results show that BTO film can achieve 180° folding and its maximum bending strain is up to ~ 10%. At the same time, it is found that the BTO film can rebound and show super-elastic behavior with the removal of external force after large angle compression.

Transferring the films grown on single crystalline oxide substrates broadens the application field of the transfer-printing technology, and develops strain engineering and the applications of oxide thin films at the same time. It is worth noting that the selection of sacrificial layers and the corresponding etching solutions play crucial roles in achieving flexible inorganic oxide thin films from the epitaxial layers on single crystalline oxide substrates.

4. Conclusion

Inorganic oxides have already occupied an important position in various applications because of their rich physical properties. By achieving the flexibility of inorganic oxides films, they also show great potential in wearable devices. At present, the main approaches to the flexibility of high quality inorganic oxide film can be divided into the physical approach of mechanical peeling films from rigid substrates, and the chemical approach of transferring films from rigid substrates to flexible substrates after etching the sacrificial layer. However, there are still many problems in the preparation of stable and high-performance inorganic oxide films. In particular, typical physical approaches may rely on LLO and van der Waal epitaxy on mica. In the LLO technique, the consumption of epitaxial layer and uneven heating or cooling of the upper layer during laser irradiation may affect the performance. Van der Waal epitaxy on mica is difficult to achieve films with good stretchability. For the chemical approach, after extending the flexible technologies used in silicon-based substrates to other single crystalline oxide substrates, the selections of sacrificial layers and corresponding etching solutions should also be broadened.

Flexible inorganic oxide films and devices have exhibited great performance, and they will play key roles in the next generation of flexible wearable devices. To meet the market's requirements, the universality and practicability of methods for achieving flexible high quality inorganic oxide films should be further improved. Meanwhile, various flexible high quality inorganic oxide films should be integrated for practical applications. With the rapid development of materials, mechanics, manufacturing science and the rise of flexible devices, people are increasingly looking forward to the application of inorganic oxide functional films in flexible devices. This can not only greatly reduce the size of traditional devices, which will hopefully break Moore's law and greatly improve device performance, but can also expand the application field of flexible devices. At the same time, the development of inorganic oxides in rigid devices has matured and it is bound to accelerate with the development of flexible devices. Because the core of realizing inorganic oxide thin film flexible devices is to realize flexible inorganic oxide thin film, getting free-standing or self-supporting inorganic oxide thin film and realizing the integration of inorganic oxide thin film on flexible substrates have become the research focus. It is believed that flexible, high quality, inorganic oxide films and devices will promote the development of flexible wearable devices, and make our life more efficient and convenient in the electronic information era.

Acknowledgements

References

[1]   Choi K J, Biegalski M, Li Y L, et al. Enhancement of ferroelectricity in strained BaTiO$_3$ thin films. Science, 2004, 306(5698), 1005

[2]   Wang C, Ke X, Wang J, et al. Ferroelastic switching in a layered-perovskite thin film. Nat Commun, 2016, 7, 10636

[3]   Lan H, Liang F, Jiang X, et al. Pushing nonlinear optical oxides into the mid-infrared spectral region beyond 10 μm: design, synthesis, and characterization of La$_3$SnGa$_5$O$_{14}$. J Am Chem Soc, 2018, 140(13), 4684

[4]   Chen Z, Chen Z, Kuo C Y, et al. Complex strain evolution of polar and magnetic order in multiferroic BiFeO$_3$ thin films. Nat Commun, 2018, 9, 3764

[5]   Himcinschi C, Rix J, Röder C, et al. Ferroelastic domain identification in BiFeO$_3$ crystals using Raman spectroscopy. Sci Rep, 2019, 9, 379

[6]   Lin Y, Feng D Y, Gao M, et al. Reducing dielectric loss in CaCu$_3$Ti$_4$O$_{12}$ thin films by high-pressure oxygen annealing. J Mater Chem C, 2015, 3(14), 3438

[7]   Yao G, Gao M, Ji Y, et al. Surface step terrace tuned microstructures and dielectric properties of highly epitaxial CaCu$_3$Ti$_4$O$_{12}$ thin films on vicinal LaAlO$_3$ substrates. Sci Rep, 2016, 6, 34683

[8]   Yao G, Ji Y, Liang W, et al. Influence of vicinal surface on the anisotropic dielectric properties of highly epitaxial Ba$_{0.7}$Sr$_{0.3}$TiO$_3$ thin films. Nanoscale, 2017, 9(9), 3068

[9]   Choi M C, Kim Y, Ha C S. Polymers for flexible displays: from material selection to device applications. Prog Polym Sci, 2008, 33(6), 581

[10]   Jiang J, Bitla Y, Huang C W, et al. Flexible ferroelectric element based on van der Waals heteroepitaxy. Sci Adv, 2017, 3(6), e1700121

[11]   Ahn J H, Kim H S, Lee K J, et al. Heterogeneous three-dimensional electronics by use of printed semiconductor nanomaterials. Science, 2006, 314(5806), 1754

[12]   Yao G, Jiang D, Li J, et al. Self-activated electrical stimulation for effective hair regeneration via a wearable omnidirectional pulse generator. ACS Nano, 2019, 13(11), 12345

[13]   Yao G, Kang L, Li J, et al. Effective weight control via an implanted self-powered vagus nerve stimulation device. Nat Com-

mun, 2018, 9, 5349

[14] Yao G, Zhang H, Zhang S, et al. Highly sensitive pressure switch sensors and enhanced near ultraviolet photodetectors based on 3D hybrid film of graphene sheets decorated with silver nanoparticles. RSC Adv, 2017, 7(44), 27281

[15] Zhang S, Zhang H, Yao G, et al. Highly stretchable, sensitive, and flexible strain sensors based on silver nanoparticles/carbon nanotubes composites. J Alloys Compd, 2015, 652, 48

[16] Kim D H, Song J, Choi W M, et al. Materials and noncoplanar mesh designs for integrated circuits with linear elastic responses to extreme mechanical deformations. Proc Natl Acad Sci USA, 2008, 105(48), 18675

[17] Kim R H, Kim D H, Xiao J, et al. Waterproof AlInGaP optoelectronics on stretchable substrates with applications in biomedicine and robotics. Nat Mater, 2010, 9(11), 929

[18] Khang D Y, Jiang H, Huang Y, et al. A stretchable form of single-crystal silicon for high-performance electronics on rubber substrates. Science, 2006, 311(5758), 208

[19] Ko H C, Shin G, Wang S, et al. Curvilinear electronics formed using silicon membrane circuits and elastomeric transfer elements. Small, 2009, 5(23), 2703

[20] Mohan A M V, Kim N H, Gu Y, et al. Merging of thin- and thick-film fabrication technologies: toward soft stretchable "island-bridge" devices. Adv Mater Technol, 2017, 2(4), 1600284

[21] Xu S, Zhang Y, Jia L, et al. Soft microfluidic assemblies of sensors, circuits, and radios for the skin. Science, 2014, 344(6179), 70

[22] Huang Z, Hao Y, Li Y, et al. Three-dimensional integrated stretchable electronics. Nat Electron, 2018, 1(8), 473

[23] Jang K I, Li K, Chung H U, et al. Self-assembled three dimensional network designs for soft electronics. Nat Commun, 2017, 8, 15894

[24] Wong W S, Sands T, Cheung N W, et al. Fabrication of thin-film InGaN light-emitting diode membranes by laser lift-off. Appl Phys Lett, 1999, 75(10), 1360

[25] Fujii T, David A, Schwach C, et al. Micro cavity effect in GaN-based light-emitting diodes formed by laser lift-off and etch-back technique. Jpn J Appl Phys, 2004, 43(3B), L411

[26] Chu C F, Lai F I, Chu J T, et al. Study of GaN light-emitting diodes fabricated by laser lift-off technique. J Appl Phys, 2004, 95(8), 3916

[27] Li C I, Lin J C, Liu H J, et al. Van der Waal epitaxy of flexible and transparent VO_2 film on muscovite. Chem Mater, 2016, 28(11), 3914

[28] Utama M I B, Mata M D L, Magen C, et al. Twinning-, polytypism-, and polarity-induced morphological modulation in nonplanar nanostructures with van der Waals epitaxy. Adv Funct Mater, 2013, 23(13), 1636

[29] Ma C H, Lin J C, Liu H J, et al. Van der Waals epitaxy of functional MoO_2 film on mica for flexible electronics. Appl Phys Lett, 2016, 108(25), 253104

[30] Wong W S, Sands T, Cheung N W, et al. Damage-free separation of GaN thin films from sapphire substrates. Appl Phys Lett, 1998, 72(5), 599

[31] Luo J, Pohl R, Qi L, et al. Printing functional 3D microdevices by laser-induced forward transfer. Small, 2017, 13(9), 1602553

[32] Serra P, Piqué A. Laser-induced forward transfer: fundamentals and applications. Adv Mater Technol, 2018, 4(1), 1800099

[33] Fernández-Pradas J M, Sopeña P, González-Torres S, et al. Laser-induced forward transfer for printed electronics applications. Appl Phys A, 2018, 124(2), 214

[34] Sorkio A, Koch L, Koivusalo L, et al. Human stem cell based corneal tissue mimicking structures using laser-assisted 3D bioprinting and functional bioinks. Biomaterials, 2018, 171, 57

[35] Kérourédan O, Ribot E, Fricain J, et al. Magnetic resonance imaging for tracking cellular patterns obtained by laser-assisted bioprinting. Sci Rep, 2018, 8, 15777

[36] Koch L, Brandt O, Deiwick A, et al. Laser-assisted bioprinting: a novel approach for bone regeneration application. Med Sci, 2018, 34(2), 125

[37] Keriquel V, Oliveira H, Rémy M, et al. In situ printing of mesenchymal stromal cells, by laser-assisted bioprinting, for in vivo bone regeneration applications. Sci Rep, 2017, 7(1), 1778

[38] Gao Y, Li Y, Li R, et al. An accurate thermomechanical model for laser-driven microtransfer printing. J Appl Mech-T ASME, 2017, 84(6), 064501

[39] Luo H, Wang C, Linghu C, et al. Laser-driven programmable non-contact transfer printing of objects onto arbitrary receivers via an active elastomeric micro-structured stamp. Natl Sci Rev, 2019, 7, 296

[40] Kim S, Son J H, Lee S H, et al. Flexible crossbar-structured resistive memory arrays on plastic substrates via inorganic-based laser lift-off. Adv Mater, 2014, 26(44), 7480

[41] Lee H E, Kim S, Ko J, et al. Skin-like oxide thin-film transistors for transparent displays. Adv Funct Mater, 2016, 26(34), 6170

[42] Cheung Y F, Li K H, Choi H W, et al. Flexible free-standing III-nitride thin films for emitters and displays. ACS Appl Mater Interfaces, 2016, 8(33), 21440

[43] Kim T I, Jung Y H, Song J, et al. High-efficiency, microscale GaN light-emitting diodes and their thermal properties on unusual substrates. Small, 2012, 8(11), 1643

[44] Lee H E, Choi J, Lee S H, et al. Monolithic flexible vertical GaN light-emitting diodes for a transparent wireless brain optical stimulator. Adv Mater, 2018, 30(28), e1800649

[45] Kim S J, Lee H E, Choi H, et al. High-performance flexible thermoelectric power generator using laser multiscanning lift-off process. ACS Nano, 2016, 10(12), 10851

[46] Park K I, Son J H, Hwang G T, et al. Highly-efficient, flexible piezoelectric PZT thin film nanogenerator on plastic substrates. Adv Mater, 2014, 26(16), 2514

[47] Lee H S, Chung J, Hwang G T, et al. Flexible inorganic piezoelectric acoustic nanosensors for biomimetic artificial hair cells. Adv Funct Mater, 2014, 24(44), 6914

[48] Mendes M, Fu J, Porneala C, et al. Lasers in the manufacturing of LEDs. Proc SPIE, 2010, 7584, 75840T

[49] Chuang S H, Pan C T, Shen K C, et al. Thin film GaN LEDs using a patterned oxide sacrificial layer by chemical lift-off process. IEEE Photonics Technol Lett, 2013, 25(24), 2435

[50] Morimoto A, Tanimura H, Yang H, et al. Platinum film patterning by laser lift-off using hydrocarbon film on insulating substrates. Appl Phys A, 2004, 79(4–6), 1015

[51] Palneedi H, Park J H, Maurya D, et al. Laser irradiation of metal oxide films and nanostructures: applications and advances. Adv Mater, 2018, 30(14), e1705148

[52] Xu X, Liu W, Li Y, et al. Flexible mica films for high-temperature energy storage. J Materiom, 2018, 4(3), 173

[53] Ohta S I. Synthetic mica and its applications. Clay Sci, 2006, 12, 119

[54] Shen L, Liu M, Ma C, et al. Enhanced bending tuned magnetic properties in epitaxial cobalt ferrite nanopillar arrays on flexible

substrate. Mater Horiz, 2018, 5(2), 230

[55] Gao D, Tan Z, Fan Z, et al. All-inorganic flexible $Ba_{0.67}Sr_{0.33}TiO_3$ thin films with excellent dielectric properties over a wide range of frequencies. ACS Appl Mater Interfaces, 2019, 11(30), 27088

[56] Tsai M F, Jiang J, Shao P W, et al. Oxide heteroepitaxy based flexible ferroelectric transistor. ACS Appl Mater Interfaces, 2019, 11(29), 25882

[57] Quynh L T, Van C N, Tzeng W Y, et al. Flexible heteroepitaxy photoelectrode for photo-electrochemical water splitting. ACS Appl Energy Mater, 2018, 1(8), 3900

[58] Liu H J, Wang C K, Su D, et al. Flexible heteroepitaxy of $CoFe_2O_4$/muscovite bimorph with large magnetostriction. ACS Appl Mater Interfaces, 2017, 9(8), 7297

[59] Wu P C, Chen P F, Do T H, et al. Heteroepitaxy of Fe_3O_4/muscovite: a new perspective for flexible spintronics. ACS Appl Mater Interfaces, 2016, 8(49), 33794

[60] Hou W, Zhou Z, Zhang L, et al. Low-voltage-manipulating spin dynamics of flexible Fe_3O_4 films through ionic gel gating for wearable devices. ACS Appl Mater Interfaces, 2019, 11(24), 21727

[61] Liu W, Ma R, Liu M, et al. Highly stable in-plane microwave magnetism in flexible $Li_{0.35}Zn_{0.3}Fe_{2.35}O_4$ (111) epitaxial thin films for wearable devices. ACS Appl Mater Interfaces, 2018, 10(38), 32331

[62] Liu W, Liu M, Ma R, et al. Mechanical strain-tunable microwave magnetism in flexible $CuFe_2O_4$ epitaxial thin film for wearable sensors. Adv Funct Mater, 2018, 28(10), 1705928

[63] Amrillah T, Bitla Y, Shin K, et al. Flexible multiferroic bulk heterojunction with giant magnetoelectric coupling via the van der Waals epitaxy. ACS Nano, 2017, 11(6), 6122

[64] Yang Y, Yuan G, Yan Z, et al. Flexible, semitransparent, and inorganic resistive memory based on $BaTi_{0.95}Co_{0.05}O_3$ film. Adv Mater, 2017, 29(26), 1700425

[65] Gao W, You L, Wang Y, et al. Flexible $PbZr_{0.52}Ti_{0.48}O_3$ capacitors with giant piezoelectric response and dielectric tunability. Adv Electron Mater, 2017, 3(8), 1600542

[66] Liang Z, Ma C, Shen L, et al. Flexible lead-free oxide film capacitors with ultrahigh energy storage performances in extremely wide operating temperature. Nano Energy, 2019, 57, 519

[67] Liang Z, Liu M, Shen L, et al. All-inorganic flexible embedded thin film capacitors for dielectric energy storage with high performance. ACS Appl Mater Interfaces, 2019, 11(5), 5247

[68] Wu J, Liang Z, Ma C, et al. Flexible lead-free $BaTiO_3$ ferroelectric elements with high performance. IEEE Electron Device Lett, 2019, 40(6), 889

[69] Wu P C, Lin Y P, Juan Y H, et al. Epitaxial yttria-stabilized zirconia on muscovite for flexible transparent ionic conductors. ACS Appl Nano Mater, 2018, 1(12), 6890

[70] Bitla Y, Chen C, Lee H C, et al. Oxide heteroepitaxy for flexible optoelectronics. ACS Appl Mater Interfaces, 2016, 8(47), 32401

[71] Ke S, Chen C, Fu N, et al. Transparent indium tin oxide electrodes on muscovite mica for high-temperature-processed flexible optoelectronic devices. ACS Appl Mater Interfaces, 2016, 8(42), 28406

[72] Li M, Wang Y, Wang Y, et al. AZO/Ag/AZO transparent flexible electrodes on mica substrates for high temperature application. Ceram Int, 2017, 43(17), 15442

[73] Yang Y, Gao W, Xie Z, et al. An all-inorganic, transparent, flexible, and nonvolatile resistive memory. Adv Electron Mater, 2018, 4(12), 1800412

[74] Zhang Y, Cao Y, Hu H, et al. Flexible metal-insulator transitions based on van der Waals oxide heterostructures. ACS Appl Mater Interfaces, 2019, 11(8), 8284

[75] Menard E, Lee K J, Khang D Y, et al. A printable form of silicon for high performance thin film transistors on plastic substrates. Appl Phys Lett, 2004, 84(26), 5398

[76] Lee K J, J Lee J, Hwang H, et al. A printable form of single-crystalline gallium nitride for flexible optoelectronic systems. Small, 2005, 1(12), 1164

[77] Meitl M A, Zhu Z T, Kumar V, et al. Transfer printing by kinetic control of adhesion to an elastomeric stamp. Nat Mater, 2005, 5(1), 33

[78] Feng X, Meitl M A, Bowen A M, et al. Competing fracture in kinetically controlled transfer printing. Langmuir, 2007, 23(25), 12555

[79] Yan Z, Pan T, Xue M, et al. Thermal release transfer printing for stretchable conformal bioelectronics. Adv Sci, 2017, 4(11), 1700251

[80] Park K I, Lee S Y, Kim S, et al. Bendable and transparent barium titanate capacitors on plastic substrates for high performance flexible ferroelectric devices. Electrochem Solid State Lett, 2010, 13(7), G57

[81] Yao G, Pan T, Yan Z, et al. Tailoring the energy band in flexible photodetector based on transferred ITO/Si heterojunction via interface engineering. Nanoscale, 2018, 10(8), 3893

[82] Feng X, Yang B D, Liu Y, et al. Stretchable ferroelectric nanoribbons with wavy configurations on elastomeric substrates. ACS Nano, 2011, 5(4), 3326

[83] Chen L, Nagy J, M Reano R M, et al. Patterned ion-sliced lithium niobate for hybrid photonic integration on silicon. Opt Mater Express, 2016, 6(7), 2460

[84] Liang W, Gao M, Lu C, et al. Enhanced metal-insulator transition performance in scalable vanadium dioxide thin films prepared using a moisture-assisted chemical solution approach. ACS Appl Mater Interfaces, 2018, 10(9), 8341

[85] Liao F, Yan Z, Liang W, et al. Tuning the metal-insulator transition of vanadium dioxide thin films using a stretchable structure. J Alloys Compd, 2017, 705, 468

[86] Liao F, Zhu Z, Yan Z, et al. Ultrafast response flexible breath sensor based on vanadium dioxide. J Breath Res, 2017, 11(3), 036002

[87] Liao F, Lu C, Yao G, et al. Ultrasensitive flexible temperature-mechanical dual-parameter sensor based on vanadium dioxide films. IEEE Electron Device Lett, 2017, 38(8), 1128

[88] Gao M, Qi Z, Lu C, et al. Interplay between extra charge injection and lattice evolution in VO_2/$CH_3NH_3PbI_3$ heterostructure. Phys Status Solidi RRL, 2018, 12(4), 1700416

[89] Kang Z, Gao M, Lu C, et al. Thickness-modulated temperature dependent optical properties of VO_2 thin films. Appl Phys A, 2019, 125, 63

[90] Lu C, Liang W, G Min G, et al. Terahertz transmittance of cobalt-doped VO_2 thin film: investigated by terahertz spectroscopy and effective medium theory. IEEE Trans THz Sci Technol, 2019, 9(2), 177

[91] Liang W, Zhuo Z, Ji Y, et al. In-plane orientation-dependent metal-insulator transition in vanadium dioxide induced by sublattice strain engineering. npj Quantum Mater, 2019, 4, 39

[92] Fratzl P, Barth F G. Biomaterial systems for mechanosensing and actuation. Nature, 2009, 462(7272), 442

[93] Schlom D G, Chen L Q, Fennie C J, et al. Elastic strain engineering of ferroic oxides. MRS Bull, 2014, 39(2), 118

[94] Chen A, Su Q, Han H, et al. Metal oxide nanocomposites: a perspective from strain, defect, and interface. Adv Mater, 2018, 31(4), 1803241

[95] Bridoux G, Barzola-Quiquia J, Bern F, et al. An alternative route towards micro- and nano-patterning of oxide films. Nanotechnology, 2012, 23(8), 085302

[96] Bakaul S R, Serrao C R, Lee M, et al. Single crystal functional oxides on silicon. Nat Commun, 2016, 7, 10547

[97] Shen L, Wu L, Sheng Q, et al. Epitaxial lift-off of centimeter-scaled spinel ferrite oxide thin films for flexible electronics. Adv Mater, 2017, 29(33), 1702411

[98] Qi Y, Jafferis N T, Lyons K, et al. Piezoelectric ribbons printed onto rubber for flexible energy conversion. Nano Lett, 2010, 10(2), 524

[99] Qi Y, Kim J, Nguyen T D, et al. Enhanced piezoelectricity and stretchability in energy harvesting devices fabricated from buckled PZT ribbons. Nano Lett, 2011, 11(3), 1331

[100] Zhang Y, Shen L, Liu M, et al. Flexible quasi-two-dimensional CoFe$_2$O$_4$ epitaxial thin films for continuous strain tuning of magnetic properties. ACS Nano, 2017, 11(8), 8002

[101] Ji D, Cai S, Paudel T R, et al. Freestanding crystalline oxide perovskites down to the monolayer limit. Nature, 2019, 570, 87

[102] Lu D, Baek D J, Hong S S, et al. Synthesis of freestanding single-crystal perovskite films and heterostructures by etching of sacrificial water-soluble layers. Nat Mater, 2016, 15(12), 1255

[103] Wang H, Shen L, Duan T, et al. Integration of both invariable and tunable microwave magnetisms in a single flexible La$_{0.67}$Sr$_{0.33}$MnO$_3$ thin film. ACS Appl Mater Interfaces, 2019, 11(25), 22677

[104] Dong G, Li S, Yao M, et al. Super-elastic ferroelectric single-crystal membrane with continuous electric dipole rotation. Science, 2019, 366(6464), 475